Ultrasonic tracking of a rapid-exchange microcatheter with simultaneous pressure sensing for cardiovascular interventions

Sunish Mathews[1][0000-0002-2289-3669], Richard Caulfield[2][0000-0002-1430-1299],
Callum Little[1][0000-0002-2267-0924], Malcolm Finlay[3][0000-0001-6403-9340],
Adrien Desjardins[1][0000-0002-1932-1811]

[1] University College London, London, WC1E 6BT, UK
[2] Echopoint Medical, London, W1T 3JL, UK
[3] Barts Heart Centre, London, EC1A 7BE, UK
sunish.mathews@ucl.ac.uk

Abstract. Ultrasound imaging is widely used for guiding minimally invasive cardiovascular procedures such as structural heart repair and renal denervation. Visualization of medical devices such as catheters is critically important and it remains challenging in many clinical contexts. When 2D ultrasound imaging is used, the catheter can readily stray from the imaging plane; with 3D imaging, there can be a loss of visibility at steep angles of insonification. When the catheter tip is not accurately identified, there can be damage to critical structures and procedural inefficiencies. In this paper, we present a tracking system to directly visualize a custom fiber optic ultrasound sensor integrated into a rapid-exchange microcatheter, in the coordinate system of an external ultrasound imaging probe. Pairs of co-registered images were acquired in rapid succession: a tracking image obtained from the ultrasonic sensor signals that were time-synchronized to the ultrasound imaging probe transmissions, and a conventional B-mode ultrasound image. The custom fiber-optic sensor comprised a free-standing membrane originally developed for blood pressure sensing, which was optically interrogated with a wavelength-tunable laser for ultrasound reception. The measured axial and lateral tracking accuracies in water were both within the range of 0.2 to 1 mm. To obtain a preliminary indication of the clinical potential of this ultrasonic tracking system, the microcatheter was delivered over a guidewire into the femoral and renal arteries in an *in vivo* porcine model and intravascular blood pressure waveforms were obtained concurrently. The results demonstrate that ultrasonic catheter tracking using optically-interrogated fiber optic blood pressure sensors is viable, and that it could be useful to guide minimally invasive cardiovascular procedures by providing accurate, real-time position measurements.

Keywords: Ultrasound tracking, minimally invasive cardiovascular interventions, fiber optic sensing.

1   Introduction

In cardiology, endovascular microcatheters are widely used to provide sensing or interventional imaging for diagnostic and therapeutic applications. One example is a pressure-sensing microcatheter, which measures blood pressure waveforms within coronary arteries to assess the severity of a stenosis and thereby to guide decisions about stent deployment. A "rapid exchange" microcatheter has a lumen in its distal section that allows it to be delivered over a guidewire positioned within the patient's vasculature. Rapid-exchange microcatheters are typically guided to their target destination with fluoroscopic (X-ray) imaging. The use of fluoroscopic guidance has several disadvantages, including exposure of the patient and clinician to X-rays, back pain experienced by practitioners from wearing heavy X-ray protective aprons, and the need for X-ray imaging systems that are not always available in resource-constrained environments. Across a wide range of cardiovascular applications, it is of significant interest to explore alternatives to fluoroscopic guidance of microcatheters.

Ultrasound (US) tracking is an emerging method for localizing medical devices within the body that involves ultrasonic communication between the device and an external imaging system. This method can be performed in "receive-mode" with an ultrasound sensor in the device that receives transmissions from the imaging probe; the time delays between transmission and reception are processed to obtain estimates of the sensor position in 2D [1, 2] and 3D [3, 4]. In reciprocal "transmit-mode" US tracking, the imaging probe receives transmissions from the device [5]. Fiber optic receivers are well suited to receive-mode US tracking: they have broad bandwidth for compatibility with different imaging probes and for high tracking resolution, they are largely omnidirectional, and their small lateral dimensions and flexibility are well suited to integration into minimally invasive cardiovascular devices such as microcatheters. Previous studies with fiber optic receivers have been focused on tracking needles, for instance in the contexts of peripheral nerve blocks and fetal medicine [2, 6].

US tracking of microcatheters would potentially enable ultrasound imaging to be used in place of X-ray imaging for guidance, particularly in applications where there are unobstructed ultrasonic views of the vasculature; these devices typically have very low echogenicity due to their small dimensions and polymeric construction. To the authors' knowledge, US microcatheter tracking has not previously been performed. This endeavor leads to several questions that are addressed in this study: first, how can a fiber optic sensor that was originally developed for blood pressure sensing be adapted to obtain concurrent ultrasound signals; second, how does spatial resolution depend on the angular orientation and spatial position of microcatheter; third, how does this combination perform within a clinically realistic environment? In this study, we address these questions, with validation in a porcine model *in vivo*.

2 Materials and Methods

2.1 Ultrasonic Tracking and Concurrent Pressure Sensing System

The ultrasonic tracking system comprised three components: a clinical US imaging system (SonixMDP, Ultrasonix, Canada) with an external 2-D linear array probe (L14-5; 128 elements), a coronary microcatheter with the integrated pressure/ultrasound sensor (as described in Section 2.2), and an US tracking console. The tracking console interrogated the fiber optic sensor in the microcatheter to receive transmissions from the array probe, and obtained processed B-mode US images and two triggers (start of each B-mode frame; start of each A-line) from the US imaging system.

The US signals received by the fiber optic sensor were parsed according to the onsets of the A-lines using the acquired triggers, and concatenated to create a 2-D tracking image of the sensor that was inherently co-registered to the corresponding B-mode US images. Envelope detection of the US signals was performed with a Hilbert transform. To localize the sensor, a region of interest (9 mm × 9 mm) was selected from the tracking image, which was centered on the maximum value. After zeroing values less than 70% of this maximum value (an empirically-obtained threshold value), the sensor position was calculated as the location of the center of mass within this region. The coordinates of the catheter tip were then superimposed on the acquired US images frame-by-frame to show the tracked position of the catheter tip.

Automatic electronic focusing of the B-mode images was performed in order to improve the lateral tracking accuracy [7]. With this method, the estimated axial (depth) coordinate of the estimated sensor position was relayed to the US imaging system. In this way, the sensor was maintained in the electronic focus of transmissions from the imaging probe without operator intervention.

2.2 Sensor and Microcatheter

The sensor comprised a cylindrical capillary structure (diameter: 250 μm; length: 1 mm) with an inorganic membrane at the distal end. This membrane was separated by an air gap from the distal end of a single mode fiber, thereby creating a low-finesse Fabry-Pérot (F-P) cavity. As the blood pressure increases, the membrane is deflected inward, and vice-versa; this deflection is measured using phase-sensitive low-coherence interferometry with a broadband light source [8]. The sensor was integrated within a rapid-exchange coronary microcatheter (minimum/maximum diameters: 0.6 mm/0.9 mm), designed for deployment over a coronary guidewire (diameter: 0.014" = 0.36 mm). The sensor was positioned on one side of the microcatheter in the rapid-exchange region, which allowed for a guidewire to pass through the central lumen (Fig. 1). Reference pressure data were obtained from the aorta with a fluid-line and an external pressure sensor, acquired by the console synchronously with the sensor data. The sensor, microcatheter, and pressure sensing console were provided by Echopoint Medical (London, UK).

For US tracking, the sensor was interrogated concurrently with a wavelength that was continuously tuned so that the change of reflectivity with membrane deflection was maximized [9]. Light from this source was distinct from that of the broadband source used for pressure sensing, thereby avoiding optical cross-talk. The two light sources were combined using a fiber optic coupler (50/50; Thorlabs, UK). With this arrangement, invasive pressure measurements and ultrasound reception were obtained concurrently.
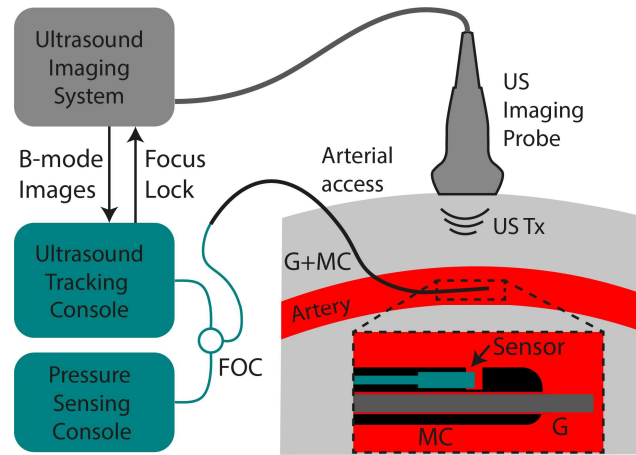
Fig. 1. Schematic of the ultrasound (US) tracking and intravascular pressure sensing system. The rapid exchange microcatheter was progressed over a guidewire within the artery; it contained a fiber optic sensor for receiving ultrasound transmissions (Tx) from the US imaging probe that was also used for concurrent intravascular pressure sensing via a fiber optic coupler (FOC). G: guidewire; MC: microcatheter.

2.3 Relative Tracking Accuracy

The relative tracking accuracy of the system was evaluated on the benchtop with the microcatheter immersed in a water tank. With the sensor and the surrounding region of the microcatheter held stationary within the imaging plane, the US imaging probe was translated in steps in the lateral and axial positions with two motorized linear translation stages (MTS50/M-Z-8, Thorlabs, UK) arranged orthogonally. At each step, 100 tracking images were acquired; a digital frequency filter (low-pass, 4th-order Butterworth; 4 MHz cut-off) was applied for noise rejection. The corresponding estimated changes in sensor position relative to the starting position were averaged. These changes were subtracted from the actual changes effected by the linear translation stages to measure the relative tracking accuracy.

2.4 Impact of Microcatheter Orientation

To determine the extent to which the hyperechoic guidewire within the central lumen of the microcatheter shadows ultrasound transmissions by the imaging probe, the signal-to-noise ratio (SNR) of the tracking signals was measured for different axial orientations. These orientations included 0°, where the sensor has a smaller depth than the guidewire and one could expect an absence of shadowing, and 180°, where the sensor has a larger depth so that the guidewire is directly above it and one could expect maximal shadowing. The catheter tip was positioned on a mount at different orientations, with the sensor in the imaging plane at a depth of the 4.5 cm. At each orientation angle, the tracking signals were recorded and the mean SNR was estimated over 100 US tracking frames. For the SNR calculation, the signal was taken as the maximum within the tracking frame; the noise was estimated as the standard deviation from deeper regions of the frame for which signals were visually absent.

2.5 *In Vivo* Validation

An initial clinical assessment of the system was performed with a swine model *in vivo*. All procedures on animals were conducted in accordance with U.K. Home Office regulations and the Guidance for the Operation of Animals (Scientific Procedures) Act (1986). Ethics approval was provided by the joint animal studies committee of the Griffin Institute and the University College London, United Kingdom.

Following arterial access, a coronary guidewire was positioned into the right femoral artery, with guidance from the external ultrasound imaging probe. The microcatheter was subsequently inserted over the guidewire and 250 US tracking frames were acquired, while the microcatheter was moved inside the artery. The microcatheter was then removed and the guidewire was positioned in a renal artery with fluoroscopic guidance. A guide catheter delivered over the guidewire allowed for injections of radio-opaque contrast for locating the renal artery. With the guide catheter removed, the microcatheter was then advanced over the guidewire into the renal artery and another 250 tracking frames were acquired with the US imaging probe mechanically fixed in position. Concurrent blood pressure data were obtained from the renal artery.

3 Results and Discussion

The relative spatial locations of the tracked and actual sensor positions in water were in good agreement for all sensor positions (Fig. 2a,b). To measure the relative axial accuracy, the depth of the sensor relative to the imaging probe (Z) was varied from 18 to 68 mm, corresponding to relative positions of 0 to 50 mm, whilst its lateral position (Y) was held in the center of the imaging plane (Y=0). Conversely, to measure lateral accuracy, Y was varied from 7 to 33 mm (full range: 0 to 38 mm), corresponding to relative positions of 0 to 26 mm, whilst Z was held constant at 68 mm. The accuracy, defined here as the absolute difference between estimated and actual relative positions, was finer in the Y dimension (< 0.6 mm) than in the Z dimension (< 0.9 mm).

The SNR of the US tracking signals varied with the orientation of the microcatheter. The axial orientation was changed from 0° to 270° in steps of 90° (Fig. 2c). The SNR was a maximum with the sensor head at 0° (SNR: 202) and a minimum at 180° (SNR: 107) (Fig. 2d). These differences in SNR can be attributed to partial US shadowing of the metallic guidewire at an orientation of 180°. Despite these shadowing effects, the SNR was sufficiently high to permit tracking at all orientations.
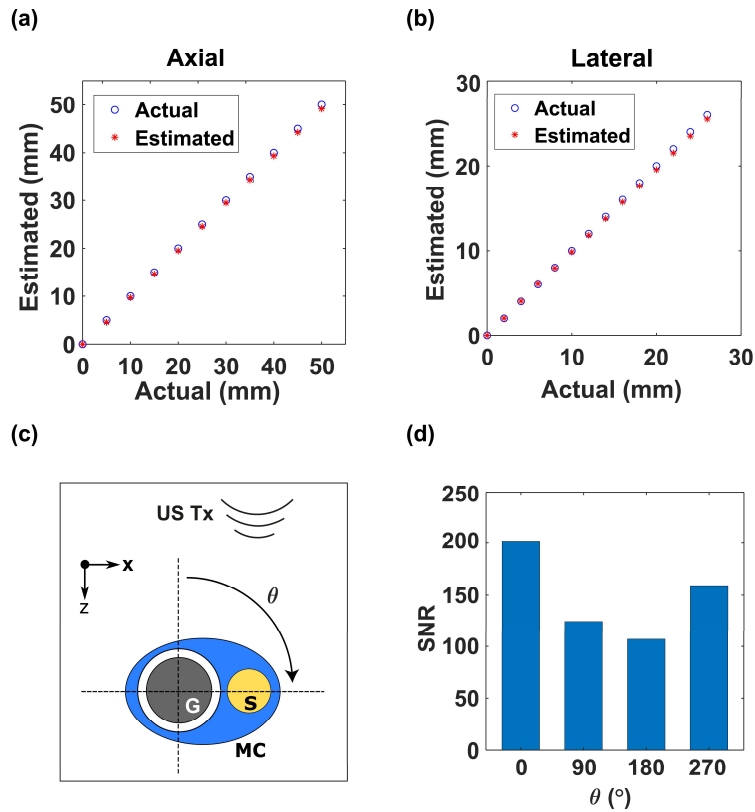
Fig. 2. Measurements of relative tracking accuracy in the axial (a) and lateral (b) directions, performed with the microcatheter and the ultrasound imaging probe in water. With a motorized translation, the axial position was increased from 18 to 68 mm, corresponding to the plotted relative axial positions of 0 to 50 mm. Likewise, the lateral position was increased from 7 to 33 mm, corresponding to the plotted relative lateral positions of 0 to 26 mm. The signal-to-noise ratio (SNR) of the tracking images was measured as a function of the angular orientation of the microcatheter (c). The region of the microcatheter (MC) containing the sensor (S) was within the imaging plane; in this cross-sectional view, the out-of-plane dimension is denoted as "x". US Tx: ultrasound transmission; G: guidewire. The SNR varied as a function of the angular orientation, assuming a maximum when the sensor was facing the imaging probe (0°) and a minimum at 180°.

When the microcatheter was in the femoral artery of the swine (depth range: 10 to 20 mm) and also in the imaging plane, SNR values as high as 72 were obtained. As the microcatheter was advanced along the guidewire inside the artery, the tracking images each had singular locations from which strong signals were obtained, which corresponded to received transmissions from the US imaging probe (Fig. 3a,b,c). During the experiment, strong visual correspondences between the estimated positions and the B-mode ultrasound images were observed.
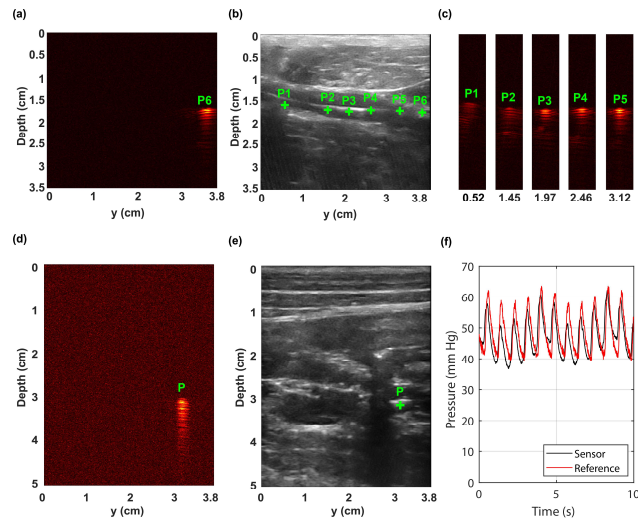
Fig. 3. Ultrasound (US) tracking of the microcatheter tip performed in a swine model *in vivo*, with the sensor within the imaging plane. (a) The tracking images contained a single, localized region of high signal corresponding to reception of ultrasound by from the imaging probe, with one example from location P6 in the femoral artery shown here. (b) As the microcatheter was progressed along the guidewire in the femoral artery with B-mode ultrasound guidance, a sequence of sensor positions (P1—P6) was estimated. (c) The signal-to-noise (SNR) ratio varied across the estimated positions P1—P5, as seen with variations in peak brightness in the laterally windowed tracking images. The values beneath the windowed images correspond to the lateral coordinates of the estimated positions. (d) The tracking images from the femoral artery are all displayed on the same linear scale. (d) This example tracking image obtained from the renal artery also had a single, localized region of high signal; however, its SNR was lower than that obtained from the femoral artery. It is plotted on a smaller linear scale than that of the tracking images from the femoral artery shown above, so that background noise is apparent. (e) The microcatheter intersected the ultrasound imaging plane only in the vicinity of the sensor. (f) Blood pressure measurements acquired concurrently with ultrasound reception for tracking showed good agreement with the reference fluid line measurement.

When the microcatheter was in the renal artery (depth range: 30 to 35 mm), SNR values as high as 19 were obtained (Fig. 3d,e). This lower maximum SNR value relative to the one obtained from the femoral artery can be attributed in part to the greater depth of the microcatheter and corresponding larger ultrasound attenuation, although slight

out-of-plane deviations from the imaging plane could also be responsible. Whilst there was axial spread in the tracking images (Fig. 3d), its impact on tracking accuracy was mitigated with the use of center of mass for sensor position estimation. The pressure trace signal recorded by the microcatheter from the renal artery was in good agreement with the reference fluid column measurement from the aorta (Fig. 3f).

To the authors' knowledge, this is the first study in which US tracking of a rapid-exchange microcatheter was performed, and also the first in which concurrent ultrasound and invasive blood pressure measurements were obtained with a single fiber optic sensor. The multimodal ultrasound/pressure sensing capability that was achieved with one optical fiber could be critically important for vessels with small lumens, to minimize the complexity, size, and flexibility of the device. With its diminutive size, this sensor could be readily incorporated into a wide range of cardiovascular devices and could find widespread utility in cardiovascular medicine. In addition to intracoronary sensing, it could be used for US tracking during endovascular repair of the tricuspid valve, where visualizing therapeutic devices with a transesophageal probe is very challenging, and during renal denervation procedures. This tracking technology is compatible with other types of US transducers than the one used here, such as curvilinear and phased array probes. Future optimizations to the sensor could include reflective surfaces on the distal end of the fiber and the pressure-sensing membrane to increase the ultrasound sensitivity via an increase in optical finesse. Upstream, diffuse delivery of light and temperature measurements from the sensor will enable invasive flow measurements [10], and optically-absorbing nanocomposite coatings applied to the distal end of the membrane could be used for concurrent optical ultrasound imaging [11]. Reproducibility of the sensor and device will be an important area of focus to broaden the range of applications for clinical translation.

The system presented here has the advantage of providing tracking images in which signals derive solely from the sensor, which are inherently co-registered with the B-mode US images. The sub-mm tracking accuracy of the system was similar to those previously obtained with receive- and transmit-mode US tracking of medical needles [1, 2]. A key observation made in this study was that high sensitivity to ultrasound transmissions could be achieved even when the microcatheter was oriented with the sensor on the opposite side of the guidewire from the imaging probe. In future studies, significant signal attenuation from adipose tissue and sound speed heterogeneities could play a confounding role. Additionally, artifacts might arise from reflections of ultrasound transmissions from strongly echoic structures such as bones or implanted medical devices, which could give rise to multiple objects in tracking images. These artifacts could be potentially mitigated using deep learning approaches developed for ultrasonic tracking [12, 13] and photoacoustic imaging [14]. Mechanical resonance of the sensor membrane, which can lead to axial spread in the tracking images, could be mitigated with frequency filtering. Ultimately, the advantages of US tracking relative to other tracking methods, including automatic image-based device detection, stereo camera tracking, electromagnetic tracking and magnetic sensing depend on a multitude of factors such as size and cost requirements. As demonstrated with an *in vivo* model in this study, ultrasonic tracking is a promising method for guiding endovascular interventions and many other minimally invasive procedures.

Acknowledgements

References

1. Baker, C., Xochicale, M., Lin, F.-Y., Mathews, S., Joubert, F., Shakir, D.I., Miles, R., Mosse, C.A., Zhao, T., Liang, W., others: Intraoperative Needle Tip Tracking with an Integrated Fibre-Optic Ultrasound Sensor. Sensors. 22, 9035 (2022).
2. Xia, W., Mari, J.M., West, S.J., Ginsberg, Y., David, A.L., Ourselin, S., Desjardins, A.E.: In-plane ultrasonic needle tracking using a fiber-optic hydrophone. Med Phys. 42, 5983–5991 (2015). https://doi.org/10.1118/1.4931418.
3. Mung, J., Vignon, F., Jain, A.: A non-disruptive technology for robust 3D tool tracking for ultrasound-guided interventions. In: Medical Image Computing and Computer-Assisted Intervention–MICCAI 2011: 14th International Conference, Toronto, Canada, September 18-22, 2011, Proceedings, Part I 14. pp. 153–160 (2011).
4. Xia, W., West, S.J., Mari, J.-M., Ourselin, S., David, A.L., Desjardins, A.E.: 3D ultrasonic needle tracking with a 1.5 D transducer array for guidance of fetal interventions. In: Medical Image Computing and Computer-Assisted Intervention–MICCAI 2016: 19th International Conference, Athens, Greece, October 17-21, 2016, Proceedings, Part I 19. pp. 353–361 (2016).
5. Xia, W., Noimark, S., Ourselin, S., West, S.J., Finlay, M.C., David, A.L., Desjardins, A.E.: Ultrasonic needle tracking with a fibre-optic ultrasound transmitter for guidance of minimally invasive fetal surgery. In: Medical Image Computing and Computer-Assisted Intervention- MICCAI 2017: 20th International Conference, Quebec City, QC, Canada, September 11-13, 2017, Proceedings, Part II. pp. 637–645 (2017).
6. Xia, W., Ginsberg, Y., West, S.J., Nikitichev, D.I., Ourselin, S., David, A.L., Desjardins, A.E.: Coded excitation ultrasonic needle tracking: An *in vivo* study. Med Phys. 43, 4065–4073 (2016).
7. Mathews, S.J., Shakir, D.I., Mosse, C.A., Xia, W., Zhang, E.Z., Beard, P.C., West, S.J., David, A.L., Ourselin, S., Vercauteren, T., others: Ultrasonic needle tracking with dynamic electronic focusing. Ultrasound Med Biol. 48, 520–529 (2022).
8. Coote, J.M., Alles, E.J., Noimark, S., Mosse, C.A., Little, C.D., Loder, C.D., David, A.L., Rakhit, R.D., Finlay, M.C., Desjardins, A.E.: Dynamic physiological temperature and pressure sensing with phase-resolved low-coherence interferometry. Opt Express. 27, 5641–5654 (2019).
9. Guggenheim, J.A., Li, J., Allen, T.J., Colchester, R.J., Noimark, S., Ogunlade, O., Parkin, I.P., Papakonstantinou, I., Desjardins, A.E., Zhang, E.Z., others: Ultrasensitive plano-concave optical microresonators for ultrasound sensing. Nat Photonics. 11, 714–719 (2017).

10. Carr, E., Mackle, E.C., Finlay, M.C., Mosse, C.A., Coote, J.M., Papakonstantinou, I., Desjardins, A.E.: Optical interferometric temperature sensors for intravascular blood flow measurements. In: European Conference on Biomedical Optics. p. 11075_1 (2019).

11. Colchester, R.J., Alles, E.J., Desjardins, A.E.: A directional fibre optic ultrasound transmitter based on a reduced graphene oxide and polydimethylsiloxane composite. Appl Phys Lett. 114, 113505 (2019).

12. Maneas, E., Hauptmann, A., Alles, E.J., Xia, W., Noimark, S., David, A.L., Arridge, S., Desjardins, A.E.: Enhancement of instrumented ultrasonic tracking images using deep learning. Int J Comput Assist Radiol Surg. 18, 395–399 (2023).

13. Maneas, E., Hauptmann, A., Alles, E.J., Xia, W., Vercauteren, T., Ourselin, S., David, A.L., Arridge, S., Desjardins, A.E.: Deep learning for instrumented ultrasonic tracking: From synthetic training data to in vivo application. IEEE Trans Ultrason Ferroelectr Freq Control. 69, 543–552 (2021).

14. Allman, D., Reiter, A., Bell, M.A.L.: Photoacoustic source detection and reflection artifact removal enabled by deep learning. IEEE Trans Med Imaging. 37, 1464–1477 (2018).